CFD modelling to study the influence of activation energy and domain size on adsorption dynamics

Muttakin, Mahbubul
International Institute for Carbon-Neutral Energy Research (WPI-I2CNER), Kyushu University | Interdisciplinary Graduate School of Engineering Sciences, Kyushu University

Mitra, Sourav
International Institute for Carbon-Neutral Energy Research (WPI-I2CNER), Kyushu University

Utami, Nadhifa Marsya
International Institute for Carbon-Neutral Energy Research (WPI-I2CNER), Kyushu University | Mechanical Engineering Department, Kyushu University

Thu, Kyaw
1International Institute for Carbon-Neutral Energy Research (WPI-I2CNER), Kyushu University | Interdisciplinary Graduate School of Engineering Sciences, Kyushu University

他

https://doi.org/10.15017/1906386

出版情報：Proceedings of International Exchange and Innovation Conference on Engineering & Sciences (IEICES). 3, pp.105-108, 2017-10-19. Interdisciplinary Graduate School of Engineering Sciences, Kyushu University
バージョン：
権利関係：

3rd International Exchange and Innovation Conference on Engineering & Sciences
Kyushu University, Fukuoka, Japan
October 19-20, 2017

CFD modelling to study the influence of activation energy and domain size on adsorption dynamics

Mahbubul Muttakin[1,2], Sourav Mitra[1], Nadhifa Marsya Utami[1,3], Kyaw Thu[1,2], Kazuhide Ito[2], Bidyut Baran Saha[1,3*]
[1]International Institute for Carbon-Neutral Energy Research (WPI-I[2]CNER), Kyushu University, 744 Motooka, Nishi-ku, Fukuoka 819-0395, Japan
[2]Interdisciplinary Graduate School of Engineering Sciences, Kyushu University, Kasuga-koen 6-1, Kasuga-shi, Fukuoka 816-8580, Japan
[3]Mechanical Engineering Department, Kyushu University, 744 Motooka, Nishi-ku, Fukuoka 819-0395, Japan
[*]Corresponding author: Tel.: +81-92-802-6722,
E-mail: saha.baran.bidyut.213@m.kyushu-u.ac.jp

Abstract: *The heat exchanger of an adsorption system comprises of an adsorber bed filled with porous granules/particles. Refrigerant vapor enters the adsorption chamber at evaporator pressure and gets adsorbed by the bed, releasing heat of adsorption. In the present study a 2-dimensional transient heat and mass transfer modeling is carried out to simulate the adsorption dynamics of ethanol on loosely packed activated carbon (Maxsorb III) bed. The model is first verified with experimental results available in literature and then utilized to observe the effects of activation energy and domain size on adsorption dynamics. The results indicate that for lower values of activation energy, the adsorption dynamics can significantly deviate from that estimated by lumped Linear Driving Force (LDF) equation. Furthermore, domain aspect ratio also plays an important role in adsorption dynamics, which can be attributed to their pressure drop characteristics.*

Keywords: Activation energy; adsorption; CFD; heat exchanger.

1. INTRODUCTION

Adsorption refrigeration has gained popularity due to its effective utilization of low grade waste heat for cooling production. This system can be run by simple flat plate or evacuated tube solar collectors, that can produce heat at a temperature of 52 to 80 °C [1,2]. The growing interest in the technology attracts scientists to do extensive research on different adsorption pairs. Research efforts have been carried out to analyze the adsorption kinetics of various adsorbent-adsorbate pairs [3–8]. El Sharkawy et al. [9] investigated the adsorption isotherm and kinetics of ethanol onto highly porous activated carbon, commercially named as Maxsorb III.
On the other side, simulation studies have been carried out by the researchers to analyze the heat and mass transfer within the adsorption heat exchanger bed [10–13]. The objective of the present study is to numerically investigate the applicability of experimentally derived kinetics parameters in designing a real adsorber bed. In order to accomplish this, ethanol-Maxsorb III pair is chosen in the current study and a simulation model is prepared in Fluent 16.0 to perform parametric analysis.

2. MODELLING

2.1 Domain

For the model a rectangular domain is chosen to simulate the adsorption process as depicted in Fig.1. Domain width (b) represents half of the fin spacing and the height (h) represents the fin height.
In the present study two different domains having the same area but different aspect ratios are taken into consideration, they are, (i) $h \times b$ = 4.5mm×2mm; and (ii) $h \times b$ = 9mm×1mm and from hereon they will be denoted by domain 1 and domain 2 respectively.

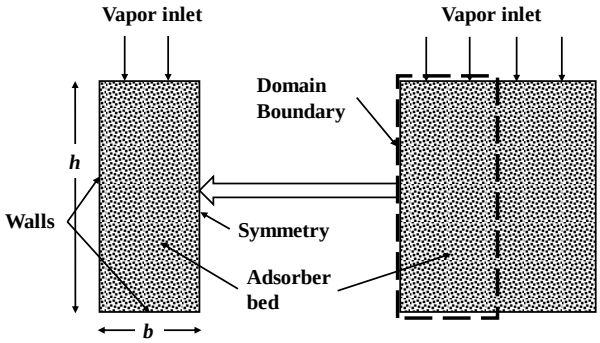

Fig. 1. Domain of the simulation model with boundary conditions.

2.2 Operating conditions

The adsorber domain is initially at a temperature of 303.15 K and that temperature is also maintained at the isothermal walls. The top of the domain experiences a pressure jump from 1.71 kPa to 2.25 kPa which initiates the adsorption process.

2.3 Assumptions

1. The walls are maintained at a constant temperature of 303.15 K.
2. Darcy model for flow through porous media is adopted.
3. Thermal equilibrium model for porous media is incorporated i.e. ethanol vapor and Maxsorb III bed are assumed to be at same temperature.
4. The bed porosity, ε and viscosity of ethanol vapor, μ are assumed to remain constant throughout the process.

5. The ethanol is assumed to behave like an ideal gas, since for the conditions in the current study, its compressibility factor is found to be 0.99.
6. The variation of heat of adsorption h_{ads} with the ethanol uptake is neglected and the average value reported by Uddin et al. [14] is used in this study.

2.4 Mathematical equations

To simulate the adsorption process, these conservation equations are modified by adding suitable source terms.

2.4.1 Equation of mass balance

$$\frac{\partial(\rho_v \varepsilon)}{\partial t}+\frac{\partial(\rho_v u)}{\partial x}+\frac{\partial(\rho_v v)}{\partial y}+\rho_{bed}\frac{\partial \phi}{\partial t}=0 \qquad (1)$$

where, u and v are the superficial velocity of ethanol vapor along x and y direction. The term $\rho_{bed}\frac{\partial \phi}{\partial t}$, is the mass sink term for vapor phase due to adsorption process.

2.4.2 Equation of momentum balance

X momentum:

$$\frac{1}{\varepsilon}\frac{\partial(\rho_v u)}{\partial t}+\frac{u}{\varepsilon^2}\frac{\partial(\rho_v u)}{\partial x}+\frac{v}{\varepsilon^2}\frac{\partial(\rho_v u)}{\partial y}= -\frac{\partial P}{\partial x}+\frac{\mu}{\varepsilon}\left(\frac{\partial^2 u}{\partial x^2}+\frac{\partial^2 u}{\partial y^2}\right)+\frac{\mu}{\lambda}u \qquad (2)$$

Y momentum:

$$\frac{1}{\varepsilon}\frac{\partial(\rho_v v)}{\partial t}+\frac{u}{\varepsilon^2}\frac{\partial(\rho_v v)}{\partial x}+\frac{v}{\varepsilon^2}\frac{\partial(\rho_v v)}{\partial y}= -\frac{\partial P}{\partial y}+\frac{\mu}{\varepsilon}\left(\frac{\partial^2 v}{\partial x^2}+\frac{\partial^2 v}{\partial y^2}\right)+\frac{\mu}{\lambda}v \qquad (3)$$

where λ represents the permeability of porous adsorbent bed given by,

$$\lambda=\frac{\varepsilon^3 d_p^2}{150(1-\varepsilon)^2} \qquad (4)$$

where d_p is the particle diameter of Maxsorb III.

2.4.3 Equation of energy balance

$$(\varepsilon\rho_v C_{p,v}+\rho_{bed}C_{p,bed})\frac{\partial T}{\partial t}+\rho_v C_{p,v}\left(u\frac{\partial T}{\partial x}+v\frac{\partial T}{\partial y}\right)= k_{eff}\left(\frac{\partial^2 T}{\partial x^2}+\frac{\partial^2 T}{\partial y^2}\right)+\rho_{bed}\frac{\partial \phi}{\partial t}h_{ads} \qquad (5)$$

The term $\rho_{bed}\frac{\partial \phi}{\partial t}h_{ads}$ is the heat source term corresponding to the heat released by adsorption process.

2.4.4 Adsorption characteristics

The Dubinin-Astakhov (D-A) adsorption isotherm equation is implemented in the model to determine the equilibrium adsorption uptake:

$$\phi^*=\phi_{\max}\exp\left[-\left\{\frac{RT}{E}\ln\left(\frac{P_s}{P}\right)\right\}^n\right] \qquad (6)$$

where ϕ^* and $\phi_{\max}$ are the equilibrium and adsorption uptake respectively. The saturation pressure P_s (in bar) is determined using the Antoine equation:

$$\log_{10} P_s=A-\frac{B}{T+C} \qquad (7)$$

The numerical values of Antoine equation parameters A, B and C for ethanol are 5.2468, 1598.673 and -46.424 respectively. To evaluate the adsorption kinetics, the widely used Linear Driving Force (LDF) equation is used in the prepared simulation model.

$$\frac{d\phi}{dt}=\frac{1}{\tau}(\phi^*-\phi) \qquad (8)$$

where, τ is the diffusion time constant given by the Arrhenius equation:

$$\frac{1}{\tau}=A\exp\left(-\frac{E_a}{RT}\right) \qquad (9)$$

A is the pre-exponential factor and is expressed by,

$$A=\frac{15D_{so}}{\left(\frac{d_p}{2}\right)^2}$$

E_a is the activation energy required to carry out the adsorption process. It is evident from equation (9) that lower the value of E_a, lower the time constant τ and hence, faster the adsorption kinetics.

The numerical values of different parameters used in the current study are presented in Table 1.

Table 1. Numerical values of simulation parameters

Parameter	Symbol	Value
Gas constant (kJ/kg K)	R	0.18
Characteristic energy for D-A equation (kJ/kg)	E	139.5
Maximum Uptake (kg/kg)	$\phi_{\max}$	1.2
Heterogeneity parameter (-)	N	1.8
Specific heat capacity of Maxsorb-III powder (kJ/kg K)	$C_{p,bed}$	0.82
Thermal conductivity (W/m K)	k_{eff}	0.066
Bed porosity (-)	ε	0.38
Packing density (kg/m^3)	ρ_{bed}	290
Skeletal density (kg/m^3)	ρ_s	2200
Heat of adsorption (kJ/kg)	h_{ads}	1002

3. Results & discussion

3.1 Model verification

A simulation model is prepared in Fluent 16.0 and the result of which is first compared with the data available in literature [9]. The experiment was conducted [9] following the same operating conditions as mentioned before. The domain size used here is $h \times b$ = 0.67mm×11.65mm.

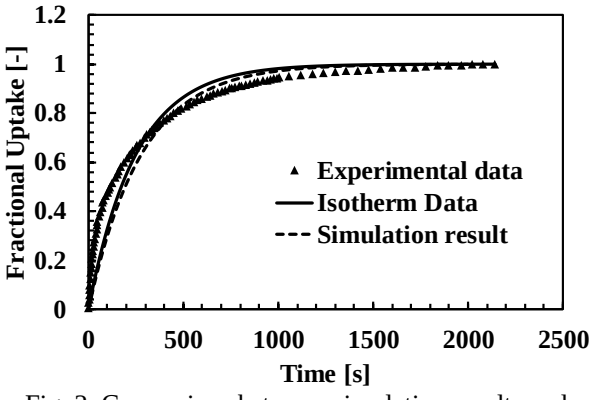

Fig. 2. Comparison between simulation results and experimental data

It is observed that the simulation results underestimate the adsorption uptake during the initial phase of adsorption and it overestimates the same after 400 s. This happened so as we used LDF equation to estimate the adsorption kinetics. Furthermore, the simulation results deviate marginally from the isotherm data, due to

heat of adsorption h_{ads} causing the temperature of the domain to vary.

3.2 Effects of domain size

Once the model is verified with the experimental data, it is utilized for the parametric analysis. As mentioned, the same operation is performed on two different domains. Domain 1 is relatively wider and shorter than domain 2.

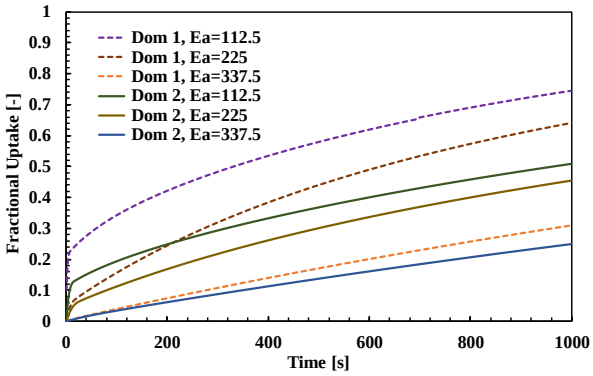

Fig. 3. Effects of domain size and activation energy on adsorption kinetics

As observed in Fig. 3, the wider domain shows better adsorption kinetics than the taller one. This phenomenon can be explained by analyzing the pressure and temperature variation within the domains, as depicted in Fig. 4. The rate of adsorption is determined by the LDF equation [equation (8)] and according to that, lower temperature lead to lower uptake. At the same time, higher pressure results in larger uptake.

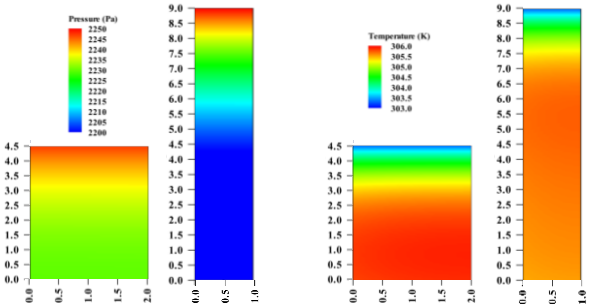

Fig. 4. Pressure and temperature contours in 2 domains after 10 s.

Assuming the 3rd dimension of the domain as unity, the taller domain has more wall surface area than the wider one; hence the dissipation of heat of adsorption is faster in domain 2. Thus, temperature of domain 1 is higher than that in domain 2. But pressure drop is also higher in taller domain as can be seen in Fig.4 and that has a pronounced effect in slowing down the adsorption uptake of that domain. Shorter domain can achieve the induced pressure almost instantaneously and that results in faster adsorption rate for domain 1 than that in domain 2.

3.3 Effects of activation energy

The activation energy estimated by El Sharkawy et al. [9] was 225 kJ/kg, which was used for the verification of the model. From the Arrhenius equation [equation (9)], we can say that lower activation energy results in faster kinetics and such is the case observed in Fig. 3. One of the objective of the current study is to analyze the effect of activation energy on the estimation of adsorption uptake using LDF equation. The LDF equation [equation (8)] can be rewritten as,

$$\frac{\phi-\phi_{in}}{\phi^{*}-\phi_{in}} = 1-\exp(-\frac{t}{\tau}) \qquad (10)$$

Where, ϕ_{in} is the initial uptake. The left side of the above equation represents fractional uptake and hence it can be stated that for LDF equation, the fractional uptake is constant for a constant value of t/τ. But from Fig. 5, it is observed that for lower values of activation energy E_a, the fractional uptake in domain 1 shows larger deviation from that estimated by LDF equation.

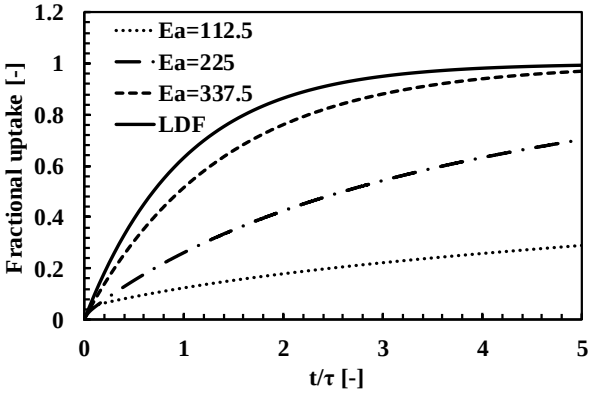

Fig. 5. Effects of activation energy on the fractional uptake for domain 1.

The reason for such deviation is, LDF equation is valid for an adsorption bed with an isothermal and isobaric conditions. This is valid for small domain volume. The assumption in using the LDF equation for the whole domain as a lumped system, leading to over prediction uptake within the domain. The effect of E_a becomes significant for lower values as it results in faster kinetics; which in turn leads to higher heat of adsorption released in a shorter period of time and hence higher temperature variation within the domain. At the same time, the pressure difference between the top and bottom regions of the domain with lower E_a value is also significant. These effects are depicted in Fig. 6 and Fig. 7. Therefore, it can be concluded that for a larger adsorber domain, typical of a real heat exchanger, the adsorption kinetics cannot be estimated from the lumped implementation of LDF equation. The temperature and pressure variation within the domain can be substantial which will affect the kinetics, but remains unaccounted if one implements the lumped form of LDF equation. The deviation increases for larger domain size or for materials with lower activation energy.

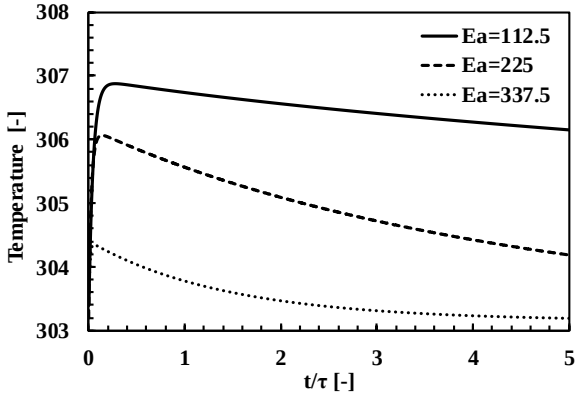

Fig. 6. Effects of activation energy on the temperature of the domain.

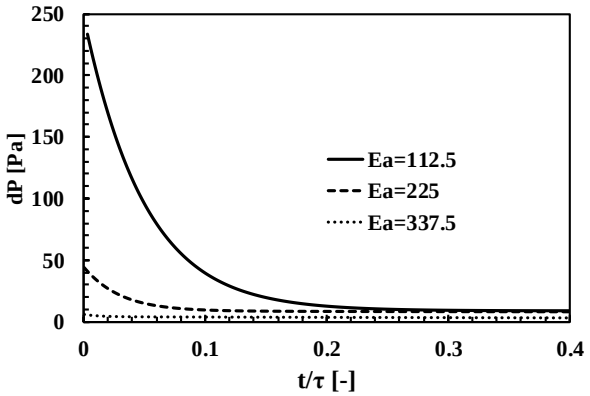

Fig. 7. Effects of activation energy on the pressure drop within the domain.

4. CONCLUSION

Numerical analysis has been performed to investigate the adsorption of ethanol onto Maxsorb III. It is found that the adsorption rate determined by the experimentally derived kinetics parameters may not be applicable in designing a real adsorption heat exchanger. Furthermore, the system capacity cannot be determined by applying lumped capacitance equations for the adsorption chamber. Activation energy can be determined in a particular domain of adsorption pair using Arrhenius equation. But in a bigger domain, as can be seen in a real adsorption heat exchanger, the kinetics may show significant deviation from that predicted by LDF equation. Because the assumption of isothermal and isobaric domain in LDF equation is not valid in a large adsorber bed.

5. REFERENCES

[1] C.A. Balaras, G. Grossman, H.-M. Henning, C.A.I. Ferreira, E. Podesser, L. Wang, E. Wiemken, Solar air conditioning in Europe—an overview, Renew. Sustain. Energy Rev. 11 (2007) 299–314.

[2] B.B. Saha, I.I. El-Sharkawy, M.W. Shahzad, K. Thu, L. Ang, K.C. Ng, Fundamental and application aspects of adsorption cooling and desalination, Appl. Therm. Eng. 97 (2016) 68–76. doi:10.1016/j.applthermaleng.2015.09.113.

[3] I.I. El-Sharkawy, B.B. Saha, S. Koyama, K.C. Ng, A study on the kinetics of ethanol-activated carbon fiber: Theory and experiments, Int. J. Heat Mass Transf. 49 (2006) 3104–3110. doi:10.1016/j.ijheatmasstransfer.2006.02.029.

[4] Y.I. Aristov, M.M. Tokarev, A. Freni, I.S. Glaznev, G. Restuccia, Kinetics of water adsorption on silica Fuji Davison RD, Microporous Mesoporous Mater. 96 (2006) 65–71. doi:10.1016/j.micromeso.2006.06.008.

[5] Y.I. Aristov, I.S. Glaznev, A. Freni, G. Restuccia, Kinetics of water sorption on SWS-1L (calcium chloride confined to mesoporous silica gel): Influence of grain size and temperature, Chem. Eng. Sci. 61 (2006) 1453–1458. doi:http://dx.doi.org/10.1016/j.ces.2005.08.033.

[6] Y. Zhong, R.E. Critoph, R.N. Thorpe, Z. Tamainot-Telto, Dynamics of BaCl2–NH3 adsorption pair, Appl. Therm. Eng. 29 (2009) 1180–1186. doi:http://dx.doi.org/10.1016/j.applthermaleng.2008.06.015.

[7] B. Dawoud, Y. Aristov, Experimental study on the kinetics of water vapor sorption on selective water sorbents, silica gel and alumina under typical operating conditions of sorption heat pumps, Int. J. Heat Mass Transf. 46 (2003) 273–281. doi:http://dx.doi.org/10.1016/S0017-9310(02)00288-0.

[8] J. V Veselovskaya, R.E. Critoph, R.N. Thorpe, S. Metcalf, M.M. Tokarev, Y.I. Aristov, Novel ammonia sorbents “porous matrix modified by active salt” for adsorptive heat transformation: 3. Testing of “BaCl2/vermiculite” composite in a lab-scale adsorption chiller, Appl. Therm. Eng. 30 (2010) 1188–1192. doi:http://dx.doi.org/10.1016/j.applthermaleng.2010.01.035.

[9] I.I. El-Sharkawy, K. Uddin, T. Miyazaki, B.B. Saha, S. Koyama, J. Miyawaki, S.H. Yoon, Adsorption of ethanol onto parent and surface treated activated carbon powders, Int. J. Heat Mass Transf. 73 (2014) 445–455. doi:10.1016/j.ijheatmasstransfer.2014.02.046.

[10] S. Jribi, T. Miyazaki, B.B. Saha, S. Koyama, S. Maeda, T. Maruyama, Corrected adsorption rate model of activated carbon–ethanol pair by means of CFD simulation, Int. J. Refrig. 71 (2016) 60–68. doi:10.1016/j.ijrefrig.2016.08.004.

[11] H. Niazmand, I. Dabzadeh, Numerical simulation of heat and mass transfer in adsorbent beds with annular fins, Int. J. Refrig. 35 (2012) 581–593. doi:10.1016/j.ijrefrig.2011.05.013.

[12] M. Mahdavikhah, H. Niazmand, Effects of plate finned heat exchanger parameters on the adsorption chiller performance, Appl. Therm. Eng. 50 (2013) 939–949. doi:10.1016/j.applthermaleng.2012.08.033.

[13] A. Chakraborty, B.B. Saha, Y.I. Aristov, Dynamic behaviors of adsorption chiller: Effects of the silica gel grain size and layers, Energy. 78 (2014) 304–312. doi:10.1016/j.energy.2014.10.015.

[14] K. Uddin, I.I. El-Sharkawy, T. Miyazaki, S. Koyama, H.-S. Kil, J. Miyawaki, S.-H. Yoon, Adsorption characteristics of ethanol onto functional activated carbons with controlled oxygen content, Appl. Therm. Eng. 72 (2014) 211–218. doi:10.1016/j.applthermaleng.2014.03.062.